



HAL
open science

Halo-tellurite glass fiber with low OH content for 2-5 μ m mid-infrared nonlinear applications

Feng Xian, Shi Jindan, Martha Segura, Nicolas M. White, Pradeesh Kannan, Wei H. Loh, Laurent Calvez, Xianghua Zhang, Laurent Brilland

► **To cite this version:**

Feng Xian, Shi Jindan, Martha Segura, Nicolas M. White, Pradeesh Kannan, et al.. Halo-tellurite glass fiber with low OH content for 2-5 μ m mid-infrared nonlinear applications. *Optics Express*, 2013, 21 (16), pp.18949-18954. 10.1364/OE.21.018949 . hal-00858277

HAL Id: hal-00858277

<https://univ-rennes.hal.science/hal-00858277>

Submitted on 6 Sep 2013

HAL is a multi-disciplinary open access archive for the deposit and dissemination of scientific research documents, whether they are published or not. The documents may come from teaching and research institutions in France or abroad, or from public or private research centers.

L'archive ouverte pluridisciplinaire **HAL**, est destinée au dépôt et à la diffusion de documents scientifiques de niveau recherche, publiés ou non, émanant des établissements d'enseignement et de recherche français ou étrangers, des laboratoires publics ou privés.

Halo-tellurite glass fiber with low OH content for 2-5 μ m mid-infrared nonlinear applications

Xian Feng,^{1,*} Jindan Shi,¹ Martha Segura,¹ Nicolas M. White,¹ Pradeesh Kannan,¹
Wei H. Loh,¹ Laurent Calvez,² Xianghua Zhang,² and Laurent Brilland³

¹Optoelectronics Research Centre, University of Southampton, Southampton, SO17 1BJ, UK

²Laboratory of Glasses and Ceramics, University of Rennes I, France

³PERFOS; R&D platform of Photonics Bretagne, France

*xif@orc.soton.ac.uk

Abstract: We report the fabrication of new dehydrated halo-tellurite glass fibers with low OH content (1ppm in weight) and low OH-induced attenuation of 10dB/m in 3-4 μ m region. It shows halo-tellurite glass fibers a promising candidate for nonlinear applications in 2-5 μ m region.

©2013 Optical Society of America

OCIS codes: (060.2290) Fiber materials; (060.4370) Nonlinear optics, fibers.

References and links

1. A. Schliesser, N. Picqué, and T. W. Hänsch, "Mid-infrared frequency combs," *Nature Photon.* **6**, 440–449, (2012).
2. P. St. J. Russell, "Photonic crystal fibers," *Science* **299**, 358–362 (2003).
3. J. K. Ranka, R. S. Windeler, and A. J. Stentz, "Visible continuum generation in air-silica microstructure optical fibers with anomalous dispersion at 800 nm," *Opt. Lett.* **25**, 25–27 (2000).
4. D. K. Serkland, and P. Kumar, "Tunable fiber-optic parametric oscillator," *Opt. Lett.* **24**(2), 92-94 (1999).
5. S. T. Cundiff, and J. Ye, "Colloquium: Femtosecond optical frequency combs," *Rev. Mod. Phys.* **75**(1), 325-342 (2003).
6. B. Szigeti, "Polarisability and dielectric constant of ionic crystals," *Trans. Faraday Soc.* **45**, 155-166 (1949).
7. J. Y. Boniort, C. Brehm, P. H. DuPont, D. Guignot, and C. Le Sergent, "Infrared glass optical fibers for 4 and 10 micron bands," *Proc. 6th ECOC York (London: IEE, 1980)* 61-64 (1980).
8. M. Poulain, M. Poulain, J. Lucas, and P. Brun, "Verres fluores au tetrafluorure de zirconium proprietes optiques d'un verre dope au Nd³⁺," *Mat. Res. Bull.* **10**, 243–246 (1975).
9. N. S. Kapany and R. J. Simms, "Recent developments of infrared fiber optics," *Infrared Phys.* **5**, 69–75 (1965).
10. J. S. Wang, E. M. Vogel, and E. Snitzer, "Tellurite glass: a new candidate for fiber devices," *Opt. Mater.* **3**, 187-203 (1994).
11. G. Ghosh, "Sellmeier coefficients and chromatic dispersions for some tellurite glasses," *J. Am. Ceram. Soc.* **78**, 2828-30 (1995).
12. X. Feng, W. H. Loh, J. C. Flanagan, A. Camerlingo, S. Dasgupta, P. Petropoulos, P. Horak, K. E. Frampton, N. M. White, J. H. V. Price, H. N. Rutt, and D. J. Richardson, "Single-mode tellurite glass holey fiber with extremely large mode area for infrared nonlinear applications," *Opt. Express* **16**(18), 13651-13656 (2008).
13. P. Domachuk, N. A. Wolchover, M. Cronin-Golomb, A. Wang, A. K. George, C. M. B. Cordeiro, J. C. Knight, and F. G. Omenetto, "Over 4000 nm bandwidth of mid-IR supercontinuum generation in sub-centimeter segments of highly nonlinear tellurite PCFs," *Opt. Express* **16**(10), 7161-7168 (2008).
14. O. Humbach, H. Fabian, U. Grzesik, U. Haken, and W. Heitmann, "Analysis of OH absorption bands in synthetic silica," *J. Non-Crystall. Solids* **203**(1), 19–26 (1996).
15. P. W. France, S. F. Carter, J. R. Williams, K. J. Beales, and J. M. Parker, "OH-absorption in fluoride glass infra-red fibres," *Electron. Lett.* **20**(14), 607-608 (1984).
16. X. Feng, S. Tanabe, and T. Hanada, "Hydroxyl groups in erbium-doped germanotellurite glasses," *J. Non-Crystall. Solids* **281**(1-3), 48–54 (2001).
17. A. E. Comyns (Ed.) *Fluoride glasses*, (John Wiley & Sons) (1989).
18. S. Nagel, J. B. MacChesney, and K. Walker, "An overview of the modified chemical vapor deposition (MCVD) process and performance," *IEEE J. Quan. Electron.* **18**(4), 459 – 476 (1982).
19. M. D. O'Donnell, C. A. Miller, D. Furniss, V. K. Tikhomirov, and A. B. Seddon, "Fluorotellurite glasses with improved mid-infrared transmission," *J. Non-Crystall. Solids* **331**(1–3), 48–57 (2003).

20. H. Ebendorff-Heidepriem, K. Kuan, M. R. Oermann, K. Knight, and T. M. Monro, "Extruded tellurite glass and fibers with low OH content for mid-infrared applications," *Opt. Mater. Express* **2**(4), 432-442 (2012).
21. N. L. Boling, A. J. Glass, and A. Owyong, "Empirical relationships for predicting non-linear refractive-index changes in optical solids," *IEEE J. Quan. Electron.* **QE-14**, 601-608 (1978).
22. K. M. Kiang, K. Frampton, T.M. Monro, R. Moore, J. Tucknott, D. W. Hewak, D. J. Richardson, and H. N. Rutt, "Extruded single-mode non-silica glass holey optical fibres," *Electron. Lett.* **38**(12), 546-547 (2002).
23. J. Shi, X. Feng, P. Horak, K. K. Chen, P. S. Teh, S.-U. Alam, W. H. Loh, D. J. Richardson, and M. Ibsen, "1.06 μm picosecond pulsed, normal dispersion pumping for generating efficient broadband infrared supercontinuum in meter-length single-mode tellurite holey fiber with high Raman gain coefficient," *J. Lightwave Technol.* **29**(22), 3461-3469 (2011).

1. Introduction

The mid-infrared (mid-IR) 2-5 μm region is one of the two atmospheric transmission windows (the second is from 8 to 13 μm) where the Earth's atmosphere is relatively transparent. It is an important area using remote laser sensing for the atmospheric, security and industrial applications such as detecting remote explosives, countermeasures against heat-seeking missiles and covert communication systems [1]. A 2-5 μm broadband or tunable laser source with medium or high average power level (100mW-10W) is thus highly demanded. Typically $\chi^{(2)}$ nonlinear crystal optical parametric oscillators (OPOs) are used for this purpose. But with such output power level and wide wavelength tunability, the size of OPO is normally large and complicated optical configurations are also required. Instead, the recent progress in dispersion tailored highly nonlinear microstructured optical fiber [2] has shown that fiber-based $\chi^{(3)}$ nonlinear laser sources, such as the supercontinuum [3], fiber OPO [4], or frequency comb [5] can also fulfil this task. What is more, fiber lasers show significant advantages over other solid state lasers as an effective approach to provide economic, compact and flexible optical components. Also excellent beam quality can be obtained from a single mode fiber.

A nonlinear glass with high transparency in 2-5 μm is required to be the host material of 2-5 μm mid-IR fiber nonlinear lasers. The position of the IR absorption edge, i.e., the infrared longwave transmission limit, of an optical glass is intrinsically limited by the multiphonon absorption edge of the glass. This can be simply explained by Hooke's law using the two-mass spring model [6]. In general, non-silica glasses, such as tellurite (TeO_2 based), fluoride (typically ZrF_4 or AlF_3 based), and chalcogenide (chalcogen S, Se, Te based) glasses [7-9], possess excellent optical transparency in the wavelength range of 0.5-5 μm , 0.4-6 μm and 1-16 μm respectively and thus are attractive candidates as fiber materials for mid-infrared applications over the conventional silica. The latter shows inferior transparency beyond 2 μm , due to (i) the strong fundamental vibration hydroxyl absorption at 2.7 μm and (ii) high loss (>50dB/m) starting from 3 μm due to the tail of the multi-phonon absorption of Si-O network.

Technically, tellurite glasses can be regarded as a high-index, highly nonlinear version of fluoride glasses. They both possess (i) steep viscosity curve around the fiber drawing temperature [10], (ii) the zero dispersion wavelength of the bulk material of $\sim 2\mu\text{m}$ [11], and (iii) longwave transmission limit (6-7 μm for bulk). But tellurite glasses have high refractive index n (2.0-2.2) and nonlinear refractive index n_2 (20-50 $\times 10^{-20}$ m^2/W), while fluoride glasses typically have n of ~ 1.5 and n_2 of $\sim 2 \times 10^{-20}$ m^2/W , as low as silica glass. Chalcogenide glass shows excellent IR transmission up to 16 μm and possesses high n_2 of 100-1000 $\times 10^{-20}$ m^2/W . However, its zero dispersion wavelength of the bulk is beyond 5 μm . In order to make a chalcogenide glass nonlinear fiber with zero dispersion wavelength close to 1.5 or 2 μm , which is the lasing wavelength of the conventional erbium or thulium doped fiber lasers, very large waveguide dispersions need to be introduced, requiring the final fiber core diameter to be submicron. This is disadvantageous for power scaling. Therefore, tellurite glasses are an ideal host material as a fiber nonlinear medium for 2-5 μm wavelength range. In principle, broadband mid-IR four-wave-mixing can be realized using a single mode large mode area tellurite fiber pumped with a high power Tm/Ho doped fiber laser [12]. But, due to the strong water absorption ($\sim 1400\text{dB/m}$) peaking at 3.4 μm , even an 8mm-long tellurite glass fiber will

suffer a 15-20dB loss in light intensity around 3-4 μm [13]. Since the tail of multiphonon absorption of tellurite glasses starts $\sim 5\mu\text{m}$, dehydration is the key approach to extend the high transmission window (i.e., absorption coefficient $< 0.1\text{cm}^{-1}$) of a tellurite glass fiber to 5 μm .

Water, commonly existing in many optical materials as the hydroxyl group OH⁻, is usually difficult to eliminate. The absorption spectrum of the OH fundamental vibration is around 3 μm and varies with the glass composition. In pure silica, the fundamental vibration of OH band is located at 2.70(± 0.02) μm and with an extinction coefficient of 10dB/m/ppm (in weight) [14], while in ZrF₄-based fluoride glass, it is located at 2.87 μm with an extinction coefficient of 5dB/m/ppm (in weight) [15]. For tellurite glass, the fundamental vibration of OH band has an extinction coefficient of $\sim 1\text{dB/m/ppm}$ (in mole) or $\sim 10\text{dB/m/ppm}$ (in weight) [16], but it is much wider than the above two glasses and ranges from 3-4 μm . This is because the large variety of deformed [TeO₄] and [TeO₃] units in tellurite glass network causes very different sites of OH groups and consequently the bond strength of OH groups shows much larger variation [16]. This is very different from the situation of pure silica glass, in which the [SiO₄] tetrahedra units are identical in the short range leading to the fundamental OH absorption as narrow as $\sim 150\text{nm}$ ($\sim 200\text{cm}^{-1}$) [14]. Since the nonlinearity n_2 of tellurite glasses is one order of magnitude higher than that of silica and fluoride glass, less than a meter length of fiber is acceptable for many nonlinear optical applications, indicating an acceptable OH peak absorption loss of no more than the level of 10dB/m. In other words, the OH impurity in a usable tellurite glass fiber should be no more than the level of 1ppm weight.

In this work, we have prepared the tellurite glass preforms in an ultradry atmosphere filled glovebox, and halide compounds are introduced into the tellurite glass compositions. The fabricated dehydrated halo-tellurite glass fibers show low OH induced attenuation from 3-4 μm , indicating that they are promising candidates for 2-5 μm nonlinear optical applications.

2. Dehydration of halo-tellurite glasses and fabrication of unclad fibers

In the case of melting glass in air, the starting chemicals are in powdered form with a large ratio of surface area to volume and the glass is easily contaminated by the moisture in the air and the OH-induced bulk attenuation of tellurite glass is typically higher than 1000dB/m [16]. An ultra-dry atmosphere is thus required for glass fabrication to obtain low OH content in the glass. Here we use an ultradry atmosphere filled glovebox with less than 0.2ppm water (in volume) for the fabrication which includes chemical batching, glass melting, preform making and annealing. A mixed N₂ and O₂ gas with the same moisture level was used as the purge in the furnace on the fiber drawing tower during the fiber drawing.

Reactive atmosphere processing (RAP) is an effective approach for dehydrating fluoride glasses [17]. During the melting of fluoride glass, dry reactive halogen gas (such as NF₃, HF, SF₆, and CCl₄) is purged into the melt to react with the OH groups inside the glass. The hydroxyl groups bonded with the glass network via hydrogen bonding are converted into the volatile compounds HF or HCl, which can be removed from the melt naturally at high temperature. Chlorine drying is also a common method in the fabrication of silica fiber preforms to reduce the OH peaks at 1.38 μm (first overtone) [18]. For tellurite glasses, in order to avoid using highly toxic and reactive halogen gases, halogen-containing solid compounds are preferable. Previously, fluorotellurite glass, obtained by introducing fluorine into the oxide tellurite glass matrix, has been proposed to remove the OH groups with the assistance of fluorine, and also to extend the mid-IR transmission [19]. However, the oxyfluoride glass has strong tendency to be crystallized easily during the heating process and hence is not a thermally stable host material for fiber drawing. Also the introduction of fluorides causes the glass hygroscopic. In addition, introducing fluorides into tellurite glasses results in significant decrease of both the refractive index and the nonlinear refractive index [19]. Here we have introduced solid-state chloride compounds, such as NaCl and PbCl₂, into the glass composition. Pyrohydrolysis reaction, $\text{OH}^- + \text{Cl}^- = \text{HCl} \uparrow + \text{O}^{2-}$, occurs during the glass melting for reducing the OH content in the glass. The compositions of the studied halo-

tellurite glasses were $75\text{TeO}_2\text{-}20\text{ZnO}\text{-}5\text{Na}_2\text{O}$ (*TZN*), $75\text{TeO}_2\text{-}20\text{ZnO}\text{-}4\text{Na}_2\text{O}\text{-}2\text{NaCl}$ (*TZNX*), and $60\text{TeO}_2\text{-}20\text{PbO}\text{-}20\text{PbCl}_2$ (*TLX*) (mol.%). Commercial chemicals with purity better than 99.999% were used as raw materials for the glass melting. For each composition, a batch of 70g was mixed well and then melted in a gold crucible inside a furnace in the glovebox at 700-900°C for 2 hours. Increasing the melting time in dry atmosphere is helpful to reduce the OH content in the glass. But it also causes the deviation of the final glass composition from the targeted one when the melting time is longer than 3 hours, since significant evaporation can be observed from tellurite glass melt. The melt was then cast in a preheated metal mold, and a bubble-free glass rod with an outer diameter (OD) of 16mm and length between 45-65mm was obtained. Fig. 1(a) shows a photograph of one of the tellurite glass rods. Each rod was drawn into an unclad fiber with an OD of 180 μm , with the yield >50m. A bulk sample was then obtained from the preform remainder with two parallel ends polished.

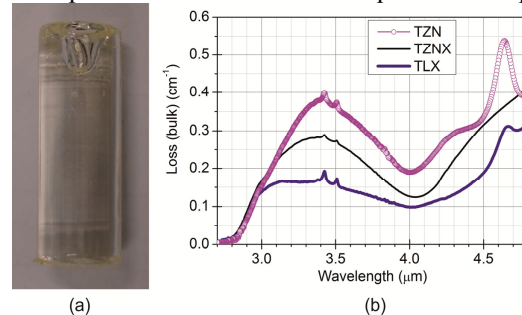


Fig. 1. (a) Optical photograph of a tellurite glass rod with 16mm OD. (b) OH-induced attenuation of dehydrated TZN, TZNX and TLX bulk glasses. Sample thickness of TZN, TZNX and TLX is 4.20mm, 8.75mm, and 2.70mm respectively.

3. Optical characteristics of dehydrated halo-tellurite bulks and fibers

The transmission spectrum of each bulk was measured by a Varian 670-IR FT-IR spectrometer. The absorption coefficient (in the unit of cm^{-1}) of the residual OH impurity in the bulk glass was calculated according to the Beer-Lambert law and converted to the bulk attenuation in dB/m. After loading the sample, dry N_2 gas was purged into the measurement chamber for at least 5 minutes to minimize the water vapor and carbon dioxide before the measurement was carried out.

Figure 1(b) shows the measured attenuation of the dehydrated tellurite glass samples. For the TZN glass, by melting in the dry atmosphere with water content less than 0.2ppm, the OH-induced loss at 3.4 μm is reduced by about one order of magnitude to 0.38cm^{-1} . This value is close to that reported in [20] by Ebendorff-Heidepriem et al., in which the TZN glass was melted in the dry atmosphere with 10ppm water content. This can be explained, because only the surface of the glass melt is dehydrated by the dry atmosphere and the convection of the melt from the inner body to the surface is fairly slow. Therefore, within about 2 hours of melting time, the amount of the OH impurity in the glass melt is weakly related to the water content in the melting atmosphere. When PbCl_2 was introduced, it is seen that the OH-induced loss is further reduced down to 0.17cm^{-1} at 3.4 μm by another factor of 2.2 in comparison with the TZN glass. The addition of NaCl did not show a dehydration effect as effective as PbCl_2 , probably because of the difference in the residual water impurity levels in the individual starting chloride materials. This can be understood from the fact that the PbCl_2 is an insoluble chloride and has much lower water solubility than NaCl. In addition, the molar percentage of the chlorine in TLX composition is 20 times higher than that in the TZNX composition and it might be another cause of such a difference. As the above formula of pyrohydrolysis reaction explains, the chlorides not only replace the OH impurity inside the glass melt, but also generate HCl vapor, which is in the bubble state from the whole glass melt and effectively stir the whole glass melt and let the whole melt have enough chance to access the interface of the

glass melt and the dry atmosphere. In addition, in Fig. 1(b) for all three curves there are two small peaks at 3.43 μm and 3.51 μm , which are artifacts arising from the protective polymer thin film coated on the optic elements in the VARIAN FTIR instrument.

A NICOLET 5700 FT-IR spectrometer (Thermo Electron Corporation) was employed for the loss measurement of the unclad TZNX and TLX fibers in the 1-4.8 μm region. On each chart in Fig. 2(a) and Fig. 2(b), the red curve for the left axis is the loss curve of the dehydrated unclad fiber; the blue curve for the right axis is the bulk loss of the glass from the same preform. The total cutback length for TZNX and TLX unclad fibers was 7cm and 52cm respectively. It is seen that the loss curves of the fiber and bulk match well with each other on the lineshape, but in the absolute value, there is a deviation with a factor of 3-7 between the bulk and the fiber. This is mainly because (i) the thickness of the bulk is not sufficiently large to give an accurate loss value when the OH loss is reduced from 1000dB/m level to 100dB/m level, and (ii) during the polishing procedure, there might be contamination from the polishing liquid on the bulk surface. On the other hand, these are not issues in the cutback loss measurement for the unclad fibers and the loss measured from the fiber should be reliable.

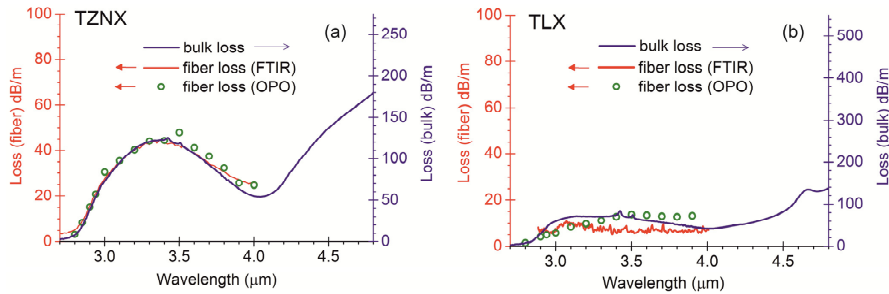


Fig. 2. Comparison of OH-induced attenuation of dehydrated (a) TZNX and (b) TLX glass unclad fibers (red curve for left axis) and bulks (blue curve for right axis).

To confirm the validity of the above statement, a crystal OPO based on 1064 nm nanosecond laser pumped magnesium oxide doped periodically lithium niobate (MgO:PPLN) (Covesion Ltd) was employed to measure the fiber loss, using the cutback method. The idler of the OPO was tuned between 2.8-4.0 μm . At each wavelength, at least 7 cutback points were measured. The total cutback length for TLX fiber was 50 - 70 cm, while for TZNX fiber it was 25 cm for 3.2 - 3.6 μm range and 40 cm for other wavelengths. From Fig. 2, it is seen that the measured fiber loss values using the OPO is close to the ones using FTIR. For each sample, at the peak wavelength the absolute difference between the fiber loss using the FTIR and the one using the OPO, is no more than 5dB/m. Note that there has been 12 months between the fiber loss measurement using the OPO and the one using FTIR, while the unclad TLX fiber has been stored in the air without special care. No significant degrading is observed in terms of the loss value. Therefore, under the dehydration process using halo-tellurite glasses containing lead chloride, the OH-induced loss at 3.4micron has been reduced down to 10dB/m, corresponding to OH levels of 1ppm weight. Compared with the previously reported lowest OH-induced loss (90-100dB/m at 3.3 μm) in tellurite glass fibers [20], our results show one order of magnitude improvement.

The refractive index of the TLX glass was measured from 0.3 to 4.0 μm , using Spectroscopic Ellipsometry between 0.3-1.7 μm and the prism method at 2.0, 3.0 and 4.0 μm . Fig. 3(a) and Fig. 3(b) show the refractive index and material dispersion curves of TLX glass from 0.3 to 5 μm , fitted by Sellmeier formula. Using the three-term Sellmeier equation $n^2(\lambda) = 1 + B_1\lambda^2/(\lambda^2 - C_1) + B_2\lambda^2/(\lambda^2 - C_2) + B_3\lambda^2/(\lambda^2 - C_3)$, in which λ is wavelength in micrometers, and B_i ($i = 1, 2, 3$) and C_i ($i = 1, 2, 3$) are the coefficients of the equation, for the TLX glass, the fitted six coefficients are B_1 : 1.212, C_1 : -6.068×10^{-2} , B_2 : 2.157, C_2 : -7.068×10^{-4} , B_3 : 0.1891, and C_3 : -45.19, respectively. Fig. 3(a) and Fig. 3(b) show the refractive index curve and the dispersion curve (0.4-3 μm) of 75TeO₂-20ZnO-5Na₂O (TZN)

respectively, according to the Sellmeier parameters of similar tellurite glasses [11]. Because the composition of TLX is very close to TZNX, their index and dispersion curves should be very close to each other. It is seen from Fig. 3(b) that the zero material dispersion wavelength of TLX glass is located at $2.30\mu\text{m}$, longer than that of TZN glass. This is useful for designing dispersion tailed mid-IR nonlinear fiber using the TLX composition.

Based on the measured refractive index, the nonlinear refractive index n_2 of TLX glass was calculated, using the well-known BGO equation [21]. The TLX glass has a high n_2 of $5.0 \times 10^{-19} \text{ m}^2/\text{W}$, about 20 times higher than that of silica glass and also higher than TZN glass ($1.7 \times 10^{-19} \text{ m}^2/\text{W}$ [12]) and the lead silicate glass Schott SF57 ($4.1 \times 10^{19} \text{ m}^2/\text{W}$ [22]).

Fig. 3(c) shows the calculated relative reduced Raman intensities of the studied tellurite glasses in comparison with a referenced pure silica glass, normalized to the peak intensity of silica at 440 cm^{-1} . The calculation procedure of relative reduced Raman intensity was described in detail in [23] by Shi et al. The TLX glass has a calculated peak Raman gain coefficient g_R of $22.6 \times 10^{-11} \text{ cm/W}$ at $1.55\mu\text{m}$, ~ 35 times higher than that of silica ($0.638 \times 10^{-11} \text{ cm/W}$), indicating the potential as a mid-IR fiber-based Raman gain medium.

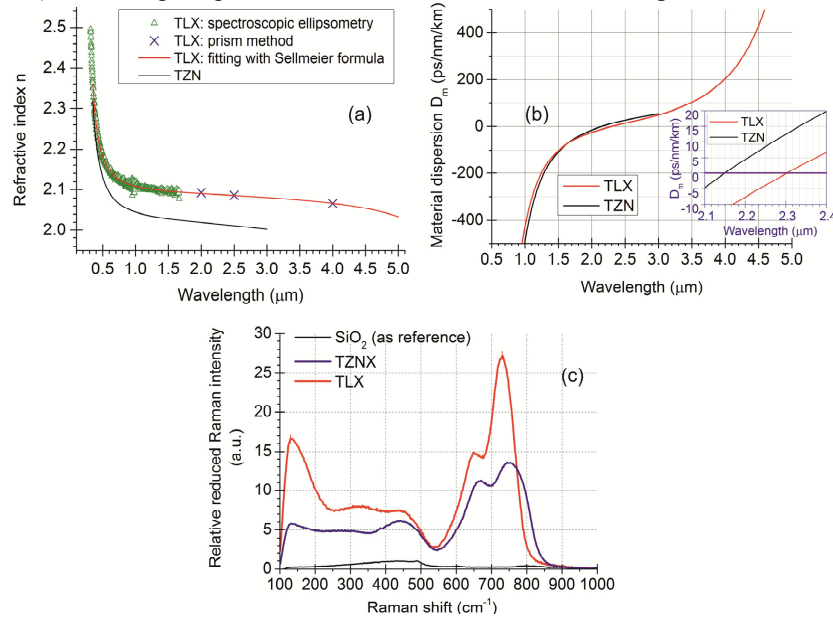


Fig. 3. (a) Refractive index and (b) dispersion curves of TZN and TLX glasses. Inset of (b): detailed curves of TZN, and TLX near their zero dispersion wavelengths. (c) Relative reduced Raman intensities of studied tellurite glasses and referenced silica

4. Conclusions

In conclusion, we report dehydrated halo-tellurite glass unclad fibers with the recorded lowest OH content (1ppm weight) and the lowest OH-induced loss (10dB/m level) in the 3-4 μm region, showing promise for nonlinear applications in 2-5 μm region. Currently the work is mainly focused on (i) further reducing the OH content down to the level 0.1ppm weight and the OH-induced loss to 1dB/m level by optimizing dehydration conditions (e.g. chlorine addition and melting time), and (ii) fabricating fibers with core/cladding structures, including hollow core fiber and small core highly nonlinear fiber for mid-IR applications.

5. Acknowledgements

This research is funded by the Engineering and Physical Sciences Research Council (UK) via the EPSRC Centre for Innovative Manufacture in Photonics and the EU FP7 CLARITY project. We also appreciate the kind assistance from Dr. James Gates and Dr. Corin Gawith for helping installing the OPO in the lab.